

Infrared surface plasmon resonance hosts for sensors

Gautam Medhi,^a Justin W. Cleary,^a Robert E. Peale,^{a*} Glenn Boreman,^a Walter R. Buchwald,^b
Sandy Wentzell,^b Oliver Edwards,^c and Isaiah Oladeji^d

^aDepartment of Physics, University of Central Florida, Orlando, Florida 32816, USA

^bAir Force Research Laboratory, Sensors Directorate, Hanscom Air Force Base, Massachusetts
01731, USA

^cZyberwear Inc., 2114 New Victor Rd., Ocoee, Florida 34761, USA

^dSisom Thin Films, LLC, 1209 West Gore Street, Orlando, FL 32805, USA

peale@mail.ucf.edu

ABSTRACT

A Surface Plasmon Resonance (SPR) biosensor that operates deep into the infrared (3-11 μm wavelengths) is potentially capable of biomolecule recognition based on both selective binding and characteristic vibrational modes. The goal is to operate such sensors at wavelengths where biological analytes are strongly differentiated by their IR absorption spectra and where the refractive index is increased by dispersion. This will provide enhanced selectivity and sensitivity, when biological analytes bind reversibly to biomolecular recognition elements attached to the sensor surface. This paper investigates potentially useful IR surface plasmon resonances hosts on lamellar gratings formed from various materials with plasma frequencies in the IR wavelength range. These materials include doped semiconductors, CuSnS, graphite and semimetal Bi and Sb. Theoretical results were compared with the experimental results. Penetration depth measurement from the experimental complex permeabilities values shows the tighter mode confinement than for usual Au giving better overlap with biological analytes.

Keywords: Biosensor, Infrared, Surface plasmon, Grating.

1. INTRODUCTION

A Surface Plasmon Resonance (SPR) biosensor for sensing bio-molecules and their interactions that operates in the infrared (3-11 μm) has potential for recognition based on both selective binding and characteristics vibrational modes. The idea is to operate specifically at wavelengths where biological analytes are strongly differentiated by their IR spectra. Established sensors are based on wavelength or angle dependent resonances in attenuated total reflection (ATR) devices using visible/near-infrared light. Selectivity might be enhanced by operating in the molecular finger print region at infrared wavelengths. Sensitivity might be increased due to dispersion enhancement of the refractive index near characteristics vibrations. SPP hosts having plasma frequencies one order less than noble metals would allow adequate overlap of IR SPP modes with biological analytes reversibly bound to the sensor surface. A sufficiently long relaxation time increases the resonance sharpness allowing small shifts in resonance angle or wavelength to be observed. Both plasma frequency and relaxation time are experimentally accessible from IR ellipsometry, and the measured complex permittivity may be used to calculate the SPP properties and SPR spectra. The proposed IR biosensor will have application in life sciences, electro analysis, drug discovery, food quality and safety, environmental science, gas and liquid phase chemical sensors, forensics, defense and security.

This paper investigates potentially useful IR SPP resonances on lamellar gratings formed from doped Si and semimetals. Heavily doped Si has been proposed by [1] with benefits discussed in [2-4]. We report here new measurements of the complex permittivity of heavily doped semiconductors Si, CuSnS and the semimetals Bi, Sb and Graphite. For Bi and Sb, the coupling resonances occur in the long wave IR near 10 μm wavelength. The resonance and surface bound electromagnetic wave exist in a region where real part of permittivity is positive ($\epsilon' > 0$) contrary to the universal assumption $\epsilon' < 0$. The IR penetration depth into the materials were calculated and compared with the calculation based on the optical constant in the wavelength region 5-11 μm . Measured SPP resonance spectra are compared with theoretical calculations.

2. EXPERIMENTAL

Bulk-doped wafers of heavily-doped p-type Si were purchased. CuSnS films were created by chemical spray deposition. A highly ordered pyrolytic graphite sample was obtained commercially from SPI Supplies. Thin films of Bi and Sb were prepared by thermal evaporation onto silicon substrates. Measurements of transmittance obtained either by

quantum cascade laser (QCL) or CO₂ laser and a Fourier spectrometer determined the skin depth in the interested IR regions. Optically thick films of Bi and Sb were then prepared by thermal evaporation for permittivity measurements. The raw ellipsometer output measured by a J.A. Woollam IR-VASE ellipsometer in the IR wavelength regions was used to calculate the complex permittivities spectrum using the standard Fresnels equation [8].

Fig. 1 presents a schematic of a grating based SPR biosensor. A monochromatic p-polarized IR light source is focused through a flow channel onto a conducting diffraction grating at an angle θ . At particular angle of incidence a surface plasmon is excited, giving a strong dip in the reflectance spectrum analyzed by an array detector. The top surface of the conducting grating is functionalized with biomolecule recognition elements that reversibly capture specific analytic biomolecules from the flow channel. This results in a refractive index change near the surface, which is sensed by the SPP field, causing a shift in the resonance angle. Lamellar gratings of 20 μm period, 50% duty cycle and different amplitude were formed by photolithography and plasma etching in silicon. The grating, suitably coated with SPP host material, was mounted on a motorized goniometer. Angular reflection spectra were obtained with a CO₂ laser operating at 9.25 and 10.59 μm wavelengths or QCL at 6.14 and 9.38 μm wavelengths.

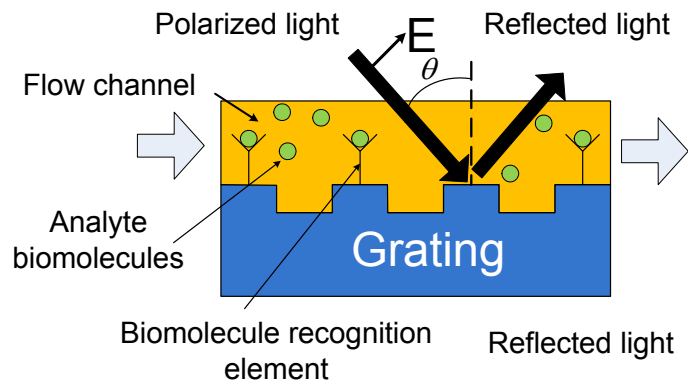
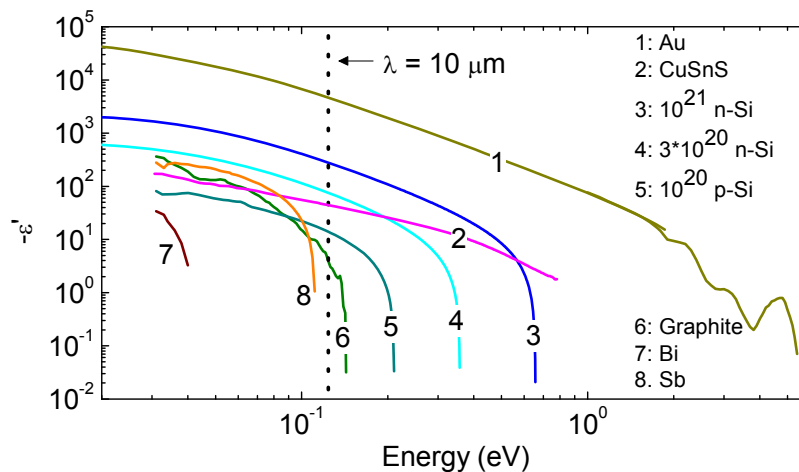


Fig. 1: Schematic of grating-based SPR biosensor

3. RESULTS

Permittivity values of different materials are presented in Fig. 2 where ϵ' is the real part and ϵ'' is the imaginary part. The n-type doped Si permittivity values are calculated values based on the Drude model for concentration 10^{21} cm^{-3} and $3 \times 10^{20} \text{ cm}^{-3}$. In our operating CO₂ wavelengths (9.25 and 10.59 μm) $\epsilon' < 0$ and $\epsilon'' > |\epsilon'|$. Permittivity values of graphite Bi, Sb and CuSnS are measured experimental values. Similarly in the same operating wavelengths $\epsilon' < 0$ and $\epsilon'' < |\epsilon'|$ for graphite whereas $\epsilon' > 0$ and $\epsilon'' > |\epsilon'|$ for Bi and Sb. Published Au permittivity values are included for comparison [5]. The wavelength of 10 μm is indicated by a vertical line. The usual requirement for SPPs is $\epsilon' < 0$.



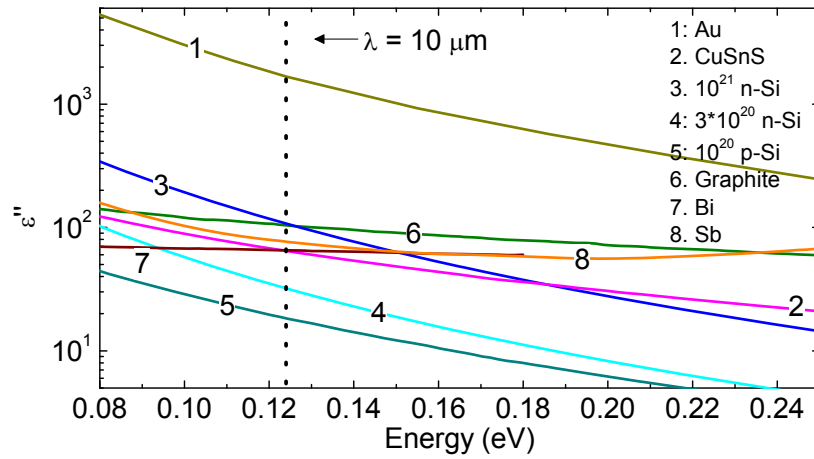


Fig. 2: Real (top) and imaginary (bottom) part of the permittivity values of n-type doped Si (10^{21} cm^{-3} and $3 \times 10^{20} \text{ cm}^{-3}$), graphite, Bi, Sb and CuSnS.

Fig. 3 presents calculated optimized resonance spectra for n-type doped Si with different carrier concentrations at the CO_2 laser wavelength of $9.25 \mu\text{m}$. To see a clear resonance, a concentration of at least 10^{20} cm^{-3} is required [6].

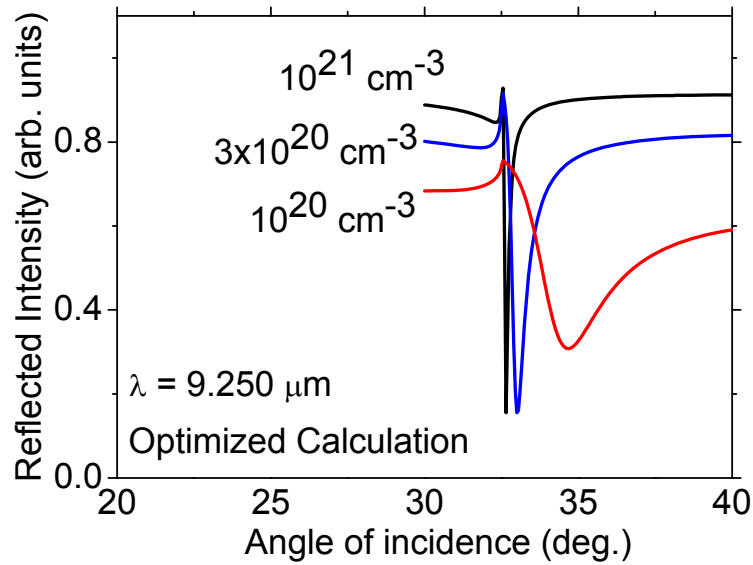


Fig. 3: Calculated reflectance spectra for n-type Si gratings with varying carrier's concentrations.

Fig. 4 shows the measured angular reflectance spectra of doped Si gratings of different amplitude etched in p-Si wafers with resistivity $0.0006\text{--}0.001 \Omega\text{-cm}$. Such material has a carrier concentration in the range $1\text{--}2 \times 10^{20} \text{ cm}^{-3}$. The measurements were done at CO_2 laser wavelength of $9.25 \mu\text{m}$ and $10.59 \mu\text{m}$ using the method described in [2]. Clear resonance spectra were observed indicating SPP excitations. The sharpest resonances occur near a grating height of $1 \mu\text{m}$, and then it starts getting broadened as $\epsilon'' > |\epsilon'|$.

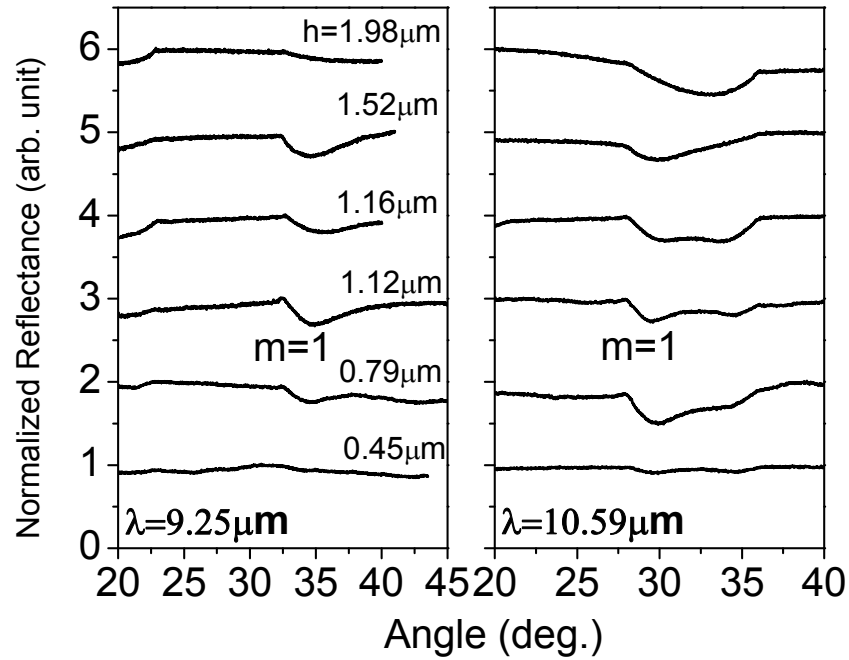


Fig. 4: Measured angular reflectance spectra of p-doped Si gratings of different amplitude measured at CO₂ wavelengths.

Fig. 5 (top) shows the optimized calculated resonances for a CuSnS grating at our QCL wavelength of 9.38 μm . The measured angular reflection spectrum of a 3 μm high CuSnS grating is presented in Fig. 5 (bottom). A resonance appears in the expected angular position, as indicated by the symbol. The grating height of 3 μm is too large for optimum SPP coupling [2], so that the measured resonance line shape agrees poorly with the optimized calculation. We expect to see a sharp resonance for a smaller grating height. The broadening of the resonance peak was also attributed due to the broadband laser.

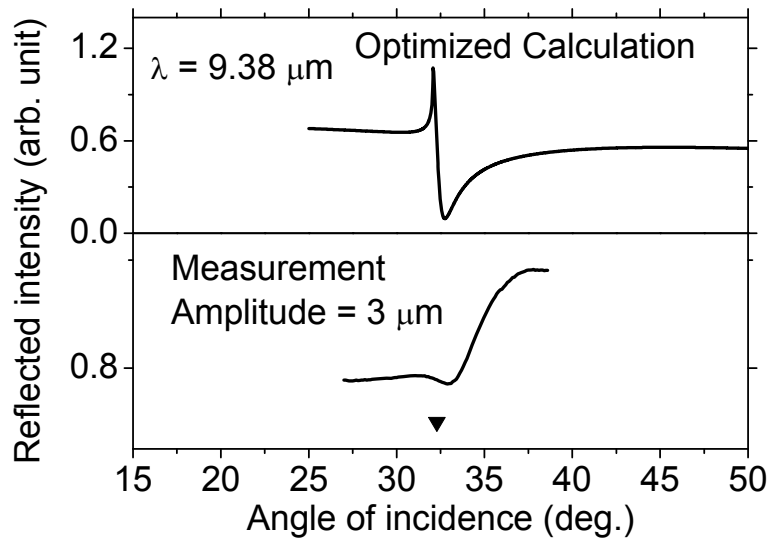


Fig. 5: Calculated reflectance spectra for a CuSnS gratings at 9.38 μm QCL wavelength (top), measured spectra of CuSnS grating of 3 μm amplitude (bottom).

The optimized calculated reflectance spectrum for a graphite grating [2] shows a reasonably sharp and deep resonance (Fig. 6, top). The calculated penetration depth for the SPP field into air above the graphite surface is 23 μm at 10 μm

wavelength. This is larger than for heavily doped Si but smaller than for silicides and noble metals. The measured angular reflectance spectrum for a 0.2 μm high graphite grating is presented in Fig. 6 (bottom). The resonances are very weak but appear near the calculated resonance angles (symbols). The grating height of 0.2 μm is too small for optimum SPP coupling [2], so that the measured resonances line shape agrees poorly with the optimized calculation.

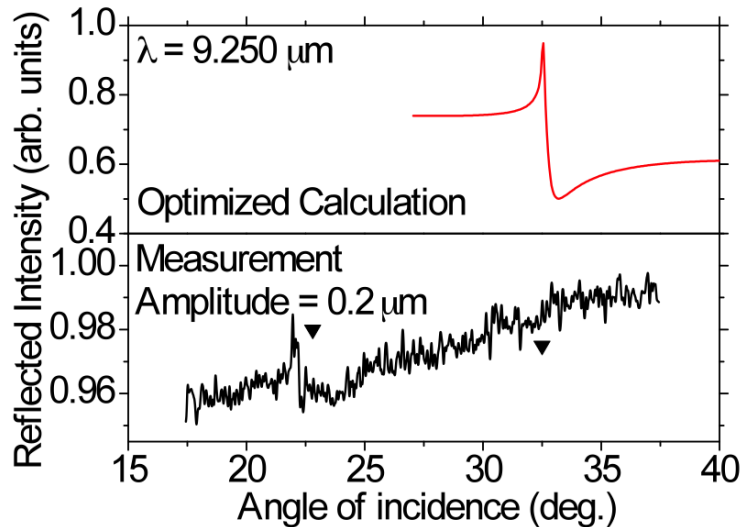


Fig. 6: Optimized calculated reflectance spectra for Graphite (top). Measured angular reflectance spectra for a graphite lamellar grating of height 0.2 μm (bottom).

Bi gratings show clear SPP resonances in calculations and in measurement. Fig. 7 (left) shows the measured reflectance spectra of Bi for different grating amplitude and wavelengths. The thin curves are the theoretical calculation. The permittivity measurement shows that a sustained SPP is possible above 30 μm wavelength when the real part of the permittivity crosses from positive to negative. This is the usual surface plasmon polariton regions. On the contrary we obtained clear resonances at our operating wavelengths. The optimal grating amplitude is 1 μm . The calculated reflectance spectra obtained from Hessel and Oliner theory [9] also shows a clear resemblance. A slightly broad resonance is due to $\epsilon'' > |\epsilon'|$ which is in contrast to the usual assumption for ordinary metals at visible wavelengths where $\epsilon'' < |\epsilon'|$. Polariton excited in this condition are called surface exciton polariton (SEP) as described in [7]. The polarization responsible is due to the movement of free electron to the surface of Bi, and hence is plasmonic in nature.

Fig 7 (right) shows the experimental resonance spectra of Sb measured at the CO_2 and QCL wavelengths at different grating amplitudes. Distinct resonances occur when the grating amplitude is at least 0.5 μm . The resonances were sharper and deeper than in Bi. The optimal grating amplitude for all the wavelength is 1 μm . The broad gain of the laser broadens the resonance at 9.38 μm . The broadening of the resonance due to laser bandwidth is negligible compared to the surface plasmon resonance linewidth for 10.59, 9.25 and 6.14 μm laser, whereas for 9.38 μm , the resonance broadening due the laser bandwidth is significant. In our measured angular range, Sb shows first ($m=1$) and third ($m=3$) resonance orders. The theoretical curve matches well with the experimental one. The calculated reflectance spectra fairly agree with the measured one. This is also the surface exciton polariton regions where $\epsilon' > 0$

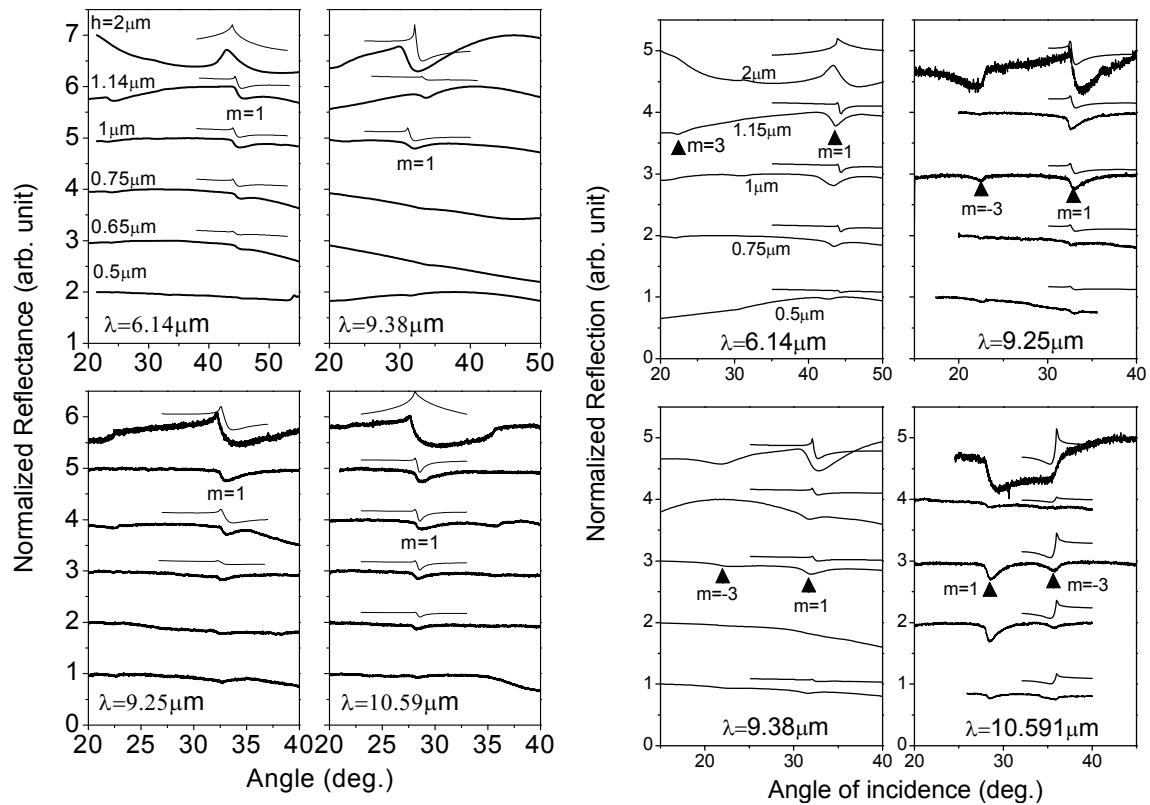


Fig. 7: Measured angular reflectance spectra of Bi (left) and Sb (right) gratings of different amplitude. Smooth curves are the calculated reflectance spectra

The calculated SPP field penetration depth above the grating surface (in our case it is air) from the permittivity values is shown in Fig. 8. The vertical line shows the energy corresponding to 10 μm wavelength. All the discussed material has a few orders of smaller penetration depth than Au at this wavelength, giving tighter mode confinement. The penetration depth has almost a linear dependency with wavelength around 10 μm for doped Si, CuSnS, and graphite whereas it shows a nonlinear behavior in Bi and Sb.

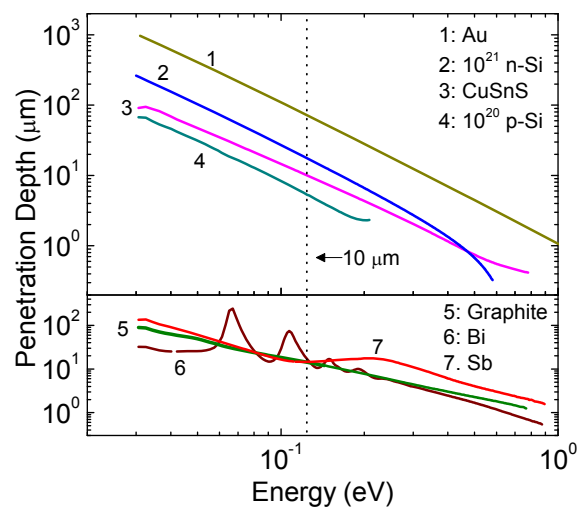


Fig. 8: SPP field penetration depth of doped Si (n and p-type), CuSnS, Graphite, Bi and Sb. The vertical line indicated the energy for 10 μm wavelength.

4. CONCLUSION

Calculated and experimental SPP resonances are presented here for materials with IR plasma frequencies. Doped Si has the sharpest SPP resonances when the doping level is high enough. Clear resonances are observed for Bi and Sb, even though the real part of the permittivity is positive at our wavelengths. Graphite and CuSnS also shows weak resonances. The SPP field penetration depth from the measured permittivity values show that these materials have tight mode confinement, thus make them promising for IR biosensor applications.

ACKNOWLEDGEMENT

This project is supported by an NSF Phase I SBIR and by an AFOSR grant FA95501010030.

REFERENCES

- [1] Chen, Y, "Development of mid-infrared surface Plasmon resonance-based sensors with highly-doped silicon for biomedical and chemical applications," *Opt. Express* **17**, 3130-3140 (2009).
- [2] Cleary, J. W., Medhi, G., Peale, R. E., and Buchwald, W. R., "Long-wave infrared surface Plasmon grating coupler", *Appl. Opt.* **49** 3102-3110 (2010).
- [3] Cleary, J., Peale, R. E., Shelton, D., Boreman, G., Soref, R., Buchwald, W., "Silicides for infrared surface plasmon resonance biosensors," *Proc. Mat. Res. Soc.* 1133-AA10-03 (2008).
- [4] Lee, K., Cho, S., Park, S. H., Heeger, A. J., Lee, C., and Lee, S., "Metallic transport in polyaniline," *Nature* **441** (2006) 65-68.
- [5] Lynch, D. W., and Hunter, W. R., "Gold (Au)," in E. D. Palik (Ed.), *Handbook of optical constants of solids*, Academic Press, Orlando, FL, 1985.
- [6] Cleary, J. W., Medhi, G., Peale, R. E., Buchwald, W. R., Edwards, O., and Oladeji, I., "Infrared surface plasmon resonance biosensor," *Proc. SPIE* 767306 (2010).
- [7] Cleary, J. W., Medhi, G., Peale, R. E., Boreman, G. D., Wentzell, S., and Buchwald, W. R., "Infrared surface polariton on antimony" (submitted 2010).
- [8] Tompkins, H.G. and Irene, E.A., "Handbook of Ellipsometry", (William Andrew, Heidelberg, 2005)
- [9] Hessel, A. and Oliner, A. A., "A new theory of Wood's anomalies on optical gratings," *Appl. Opt.* **4**, 1275-1297 (1965).